Histochemical Journal **26**, 754–763 (1994)

Nuclear pores in the apoptotic cell

ELISABETTA FALCIERI[1,2], PIETRO GOBBI[3], AMELIA CATALDI[1], LORIS ZAMAI[3], IRENE FAENZA[4] and MARCO VITALE[2,5]*

[1]*Istituto di Morfologia Umana Normale, Università di Chieti;* [2]*Istituto di Citomorfologia Normale e Patologica CNR, c/o Ist. Codivilla-Putti, Bologna;* [3]*Istituto di Anatomia Umana Normale, Università di Bologna;* [4]*Lab. Biol. Cell. Microsc. Elettr., c/o Ist. Ortopedico Rizzoli, Bologna;* [5]*Dipartimento di Scienze Biomediche e Biotecnologie, Sez. Anatomia Umana, Università di Brescia*

Received 15 March 1994 and in revised form 7 June 1994

Summary

During apoptosis, nuclear pores undergo strong modifications, which are described here in five different apoptotic models. Conventional electron microscopy, supported by freeze–fracture analysis, showed a constant migration of nuclear pores towards the diffuse chromatin areas. In contrast, dense chromatin areas appear pore-free and are frequently surrounded by strongly dilated cisternae. A possible functional significance of this pore behaviour during apoptosis is discussed.

Introduction

Apoptosis has been recognized as an apparently physiological form of cell death consisting of programmed cell deletion aimed at the maintenance of tissue homeostasis (Koury, 1992). It plays an important role during fetal development, metamorphosis and adult tissue turnover by balancing cell proliferation (Wyllie *et al.*, 1980). It frequently occurs in hormone-dependent tissues (Ellis *et al.*, 1991) as well as a consequence of treatment with various noxious agents such as toxins, anticancer drugs, microorganisms and hyperthermia (Arends & Wyllie, 1991; Ledda-Columbano *et al.*, 1991; Zychlinsky *et al.*, 1992; McCabe & Orrenius, 1992).

Apoptosis, in most cases, is related to the activation of an endogenous endonuclease activity which cleaves DNA into fragments of approximately 180 base pairs, thus generating a characteristic DNA gel electrophoretic ladder (Arends *et al.*, 1990; Fesus *et al.*, 1991; Sen & D'Incalci, 1992; Vaux, 1993). It can also be quantified by other techniques, such as flow cytometry, which demonstrates, after DNA staining, a subdiploid peak corresponding to the apoptotic cell population (Zamai *et al.*, 1993; Darzynkiewicz *et al.*, 1992), or fluorescence nick translation, which specifically stains the DNA breakpoints (De la Torre *et al.*, 1992). Recently, characteristic apoptotic patterns have been reported in different experimental models, in the absence of DNA fragmentation (Ucker *et al.*, 1992; Falcieri *et al.*, 1993; Oberhammer *et al.*, 1993). Unusual and very specific nuclear changes have long been described by ultrastructural analysis of the apoptotic cell (Wyllie *et al.*, 1980). Chromatin undergoes characteristic peripheral margination, rapidly followed by the appearance of cap-shaped electron-dense areas close to the nuclear poles, and clearly separated from the diffuse chromatin portion. Nuclear protrusions showing a deep re-arrangement of nuclear envelopes frequently appear, and lead to the formation of a variable number of uniformly electron-dense micronuclei (Vitale *et al.*, 1993). The cell, thus transformed in one or more 'apoptotic bodies', shows good preservation of the plasma membrane and organellar component which lasts for a long time, despite the severe irreversible nuclear modifications (Schwartzman & Cidlowski, 1993).

Given the central role played by nuclear pores in the nuclear cytoplasmic traffic (Nigg *et al.*, 1991), it is likely that the strong nuclear re-arrangement that takes place during apoptosis can affect their morphological appearance. In fact, nuclear pore distribution appears to be deeply altered during apoptosis, as observed by conventional electron microscopy. Here we report the distribution of nuclear pores during apoptosis in five cell lines by conventional electron microscopy and freeze–fracture, as the choice technique for investigating the ultrastructural pattern of large membrane areas.

Materials and methods

Cells

Thymocytes were obtained from two-week-old BALB/c mice (Charles River, Milano) and incubated for 24 h in RPMI 1640,

* Present address: Jefferson Cancer Inst., Bluemle Life Sciences Building, Thomas Jefferson University, Philadelphia, PA 19107, USA.

10% fetal calf serum (FCS), 10 mM Hepes buffer, 0.1 μM dexamethasone (Sigma, UK) at 37°C, as previously described (Vitale *et al.*, 1993).

TF-1 cells, a human hematopoietic progenitor cell line, were cultured in RPMI 1640, 10% FCS, 10 ng ml^{-1} IL-3 (Omnia Res, Milano), and then kept without IL-3 for 72 h to trigger apoptosis (Zamai *et al.*, 1993; Zauli *et al.*, 1994).

HL60 human leukaemia cells were routinely grown. Apoptosis was induced by the addition of 0.15 μM camptothecin (Sigma, UK) for 6 h at 37°C, 5% CO_2 (Kaufmann, 1989; Darzynkiewicz *et al.*, 1992).

Human lymphocytic leukaemia MOLT-4 cells (ATCC, Rockville, MD, USA) were cultured in RPMI 1640 and induced to apoptosis by the addition of staurosporine (Boehringer, Mannheim, Germany), as previously reported (Falcieri *et al.*, 1993).

P815 murine mastocytoma cells were routinely cultured and exposed to mild hyperthermia to induce apoptosis (Collins *et al.*, 1992).

Untreated cells were used as control specimens in the different technical procedures.

DNA gel electrophoresis

DNA was routinely extracted and purified as reported (Boe *et al.*, 1991). It was then run on a 0.8% agarose gel, as described (Falcieri *et al.*, 1993). Molecular weight markers were from Boehringer-Mannheim.

Flow cytometry

The presence of apoptotic cells after the different treatments in all cell lines used was constantly monitored by flow cytometry. Apoptosis was identified by propidium iodide (PI) incorporation after ethanol treatment in all except the MOLT-4 cell lines used (Darzynkiewicz *et al.*, 1992; Vitale *et al.*, 1993; Zauli *et al.*, 1994). Briefly, thymocytes, TF-1, HL60 and P815 were treated with 70% ethanol at 4°C for at least 30 min. Cells were then washed twice in phosphate-buffered saline (PBS), resuspended in 300 μl PBS and stained with 40 μg ml^{-1} PI (Sigma). After 10 min in the dark, samples were analysed by flow cytometry. Discrimination of the apoptotic cells from the debris was made as described by Zamai *et al.* (1993). On the contrary, apoptotic Molt-4 cells were identified in flow by their slow uptake of propidium iodide (40 μg ml^{-1}, 2 h incubation at 37°C, 5% CO_2) in the absence of ethanol treatment, as described by Vitale *et al.* (1993).

Conventional electron microscopy

After incubation, the cells were sedimented and immediately fixed with 2.5% glutaraldehyde in 0.1 M phosphate buffer. They were then post fixed with 1% OsO_4 in veronal buffer, in dehydrated ethanol and embedded in Araldite. Lowicryl K4M embedding for osmium-ammine staining of the nucleic acids was also performed (Derenzini & Farabegoli, 1990; Falcieri *et al.*, 1992).

Freeze–fracture

The same samples, prepared as separate pellets, after 2.5% glutaraldehyde fixation, were washed in the same buffer and cryoprotected in 30% glycerol in 0.1 M phosphate buffer. They were then mounted on gold supports and quickly frozen in Freon 22 and liquid nitrogen. The fracture was performed at −115°C with a Balzers BAF 400 D and platinum–carbon/carbon replicas were obtained whose thickness was checked with a quartz film monitor. Cleaning and degreasing was performed with a commercial bleach and a chloroform–methanol mixture. Formvar–carbon–coated nickel grids were used as replica supports (Falcieri *et al.*, 1990). Observations were carried out with a Philips CM10 electron microscope at 80 kV.

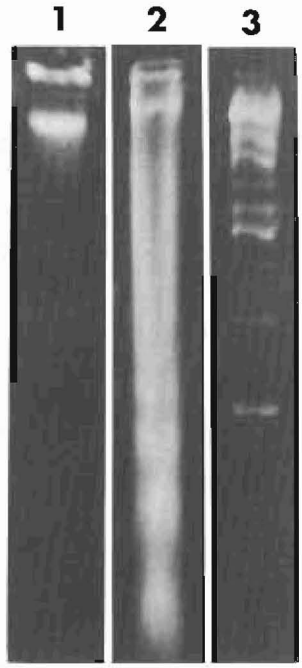

Fig. 1. DNA gel electrophoresis of camptothecin-treated (0.15 μM for 6 h) HL60 cells; 0.8% agarose gel electrophoresis of DNA from camptothecin-treated HL60 cells. Lane 1 = control cells; lane 2 = cells cultured for 6 h in the presence of (0.15 μM camptothecin); lane 3 = molecular weight marker III.

Results

After the appropriate treatment, thymocytes, TF-1, HL60 and P815 cells underwent apoptosis which could be detected by gel electrophoresis as a DNA ladder (Fig. 1), and by flow cytometry as an hypodiploid peak (Fig. 2a). In contrast, MOLT-4 cells do not produce DNA fragmentation when treated with staurosporin (Falcieri *et al.*, 1993) and, therefore, do not produce either an electrophoretic ladder or an hypodiploid peak. Fig. 2b shows the detection of apoptosis of staurosporin-treated MOLT-4 as a dimly PI-fluorescent population in flow cytometry, as described by Vitale *et al.* (1993).

Mouse thymocyte apoptosis was characteristically represented by a compact chromatin margination towards a nuclear pole. This mass appeared cap-shaped, uniformly

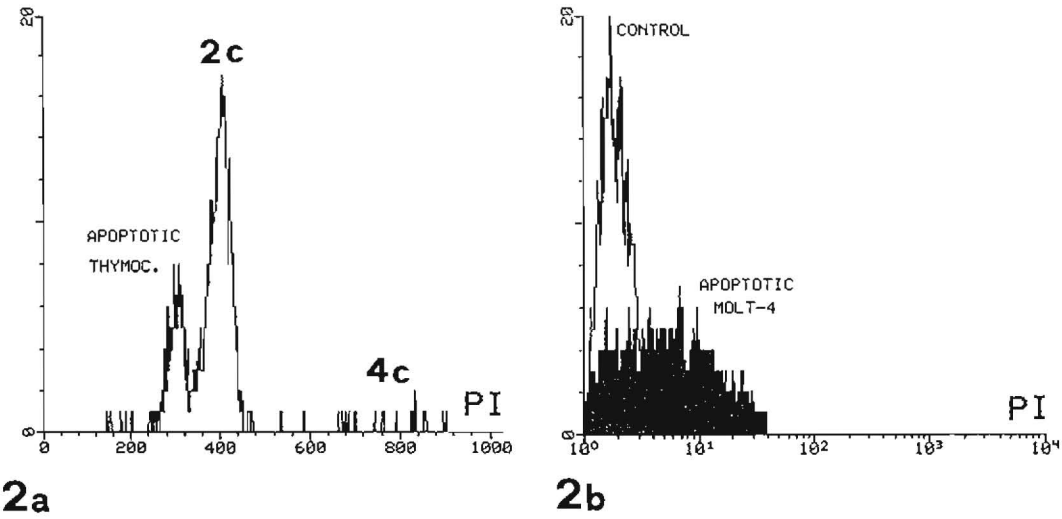

Fig. 2. PI fluorescence of mouse thymocytes treated for 24 h with 0.1 μM dexanathazone fixed in 70% ethanol. (a) Apoptosis appear as an hypodiploid peak. Similar features occurred in the TF-1, HL60 and P815 cells. X axis: linear scale of PI fluorescence signal; 2c = diploid cell subpopulation, 4c = tetraploid cell subpopulation. (b) PI fluorescence of MOLT-4 cells incubated for 2 h with 40 μg ml^{-1} PI. Overlay of untreated and staurosporin-treated samples. Dimly fluorescent cells are apoptotic. X axis: log scale of PI fluorescence signal.

electron-dense and sharply separated from the diffuse chromatin nuclear portion. A well distinguished envelope surrounded both, showing an unusual nuclear pore distribution. Pore complexes appeared to have all migrated into the diffuse chromatin areas, being entirely absent around the compact chromatin (Fig. 3a).

TF-1 cells, after IL-3 withdrawal, were induced to apoptosis and displayed similar ultrastructural patterns. Large pore-free areas adjacent to the dense chromatin also appeared in this case, the pores being concentrated around the decondensed chromatin nuclear portions (Fig. 3b). Assembling *annulate lamellae* could also be occasionally observed (Fig. 3b, inset).

Figure 3c demonstrates the unusual behaviour of the nuclear envelope, as a consequence of the irregular distribution of pores. In the areas where pores were clustered, the nuclear membranes appeared in close contact to one another and small crowded cisternae outlined the nuclear zone corresponding to the loose chromatin. However, the opposite, pore-free side was surrounded by a unique large perinuclear space. The consistent nuclear envelope dilation, frequently related to nuclear protrusions and micronuclei formation, appears as the consequence of this particular pore rearrangement. HL60 cells, when treated with camptothecin, showed similar apoptotic patterns. By conventional electron microscopy, pores clustered not only where the nuclear envelope looked at the cytoplasm but also in correspondence of neoformed nuclear protrusion (Fig. 4a). Freeze–fracture analysis of apoptotic nuclei allowed the identification of large membrane areas, with pores clustered together, clearly separated from the pore-free ones (Fig. 4b).

All nuclei observed showed a regular intramembrane particle distribution. These structures, representing the protein membrane component, are scattered throughout normal cell membranes. Their distribution is homogeneous in normal conditions but is strongly modified when membrane alterations, such as permeability changes, occur, appearing, in these cases, as particles clustered in patches (Falcieri *et al.*, 1990). Therefore, this regular pattern of membrane particle localization in apoptotic nuclei suggested a fine preservation of the nuclear membrane architecture, despite pore migration, and in both pore and pore-free areas (Fig. 4c). This was also supported by conventional electron microscopy, showing, besides the integrity of nuclear envelopes, the constant presence of ribosomes on the external membrane of the apoptotic nucleus. The unusual pore concentration in the regions connecting contiguous nuclear protrusions and/or micronuclei was also demonstrated (Fig. 5a, b). In close proximity completely pore-free micronuclei surrounded by a clearly distinguishable nuclear envelope could also be observed by freeze–fracture examination (Fig. 5b). This micronuclear polymorphism, frequently occurring in HL60 cells, can be correlated to a certain variability of nuclear volume and shape, typical of this cell line. Fig. 6a shows, in fact, a compact and a cap-shaped chromatin arrangement in two HL60 micronuclei. In the cytoplasm, some *annulate lamellae* are visible. The dimensional distribution of pores was demonstrated by freeze–fracture (Fig. 6b), showing the characteristic pore crowding at a pole of a micronucleus.

In order to investigate the relationship between pore complexes and DNA distribution more closely, we

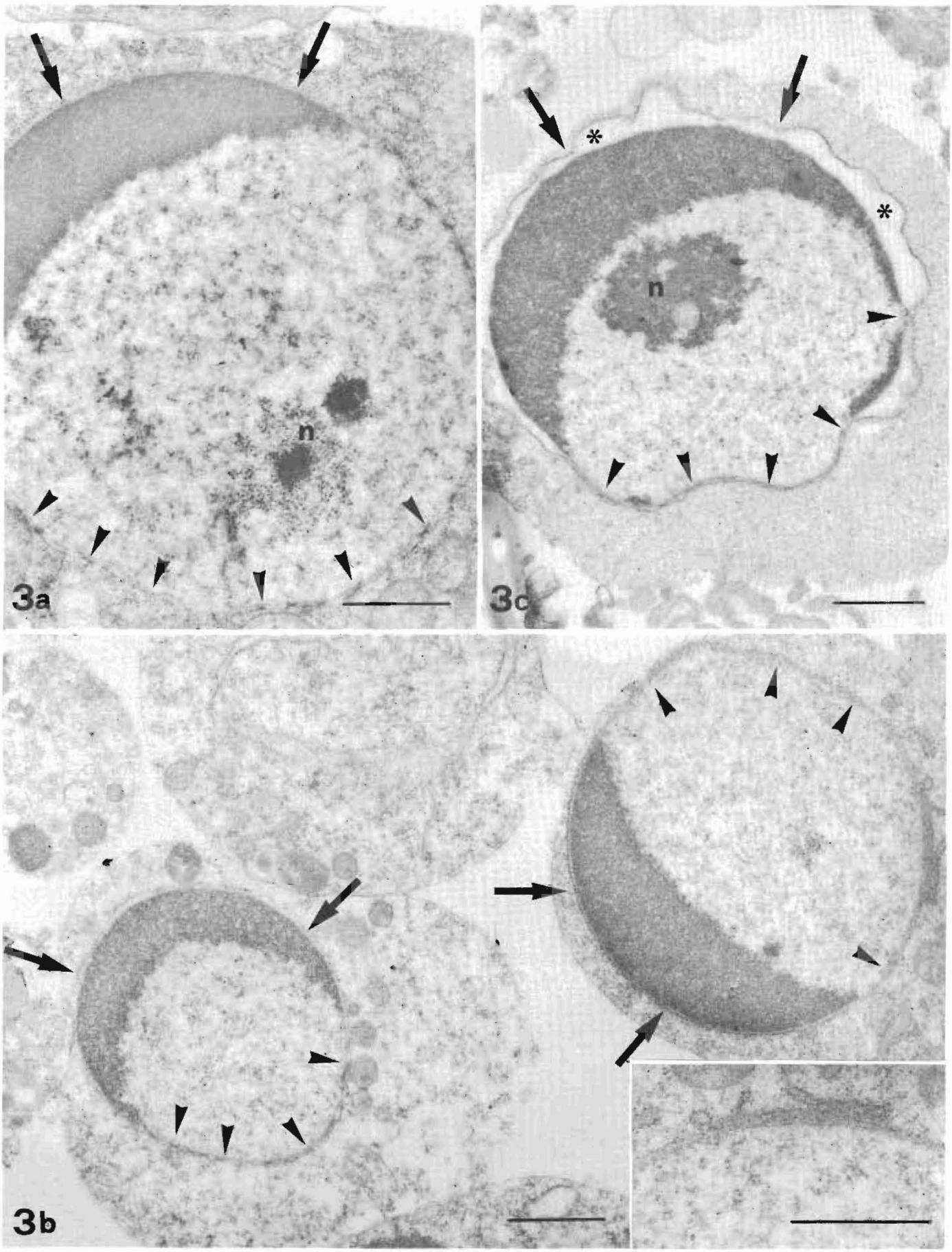

Fig. 3. *Caption on p. 759.*

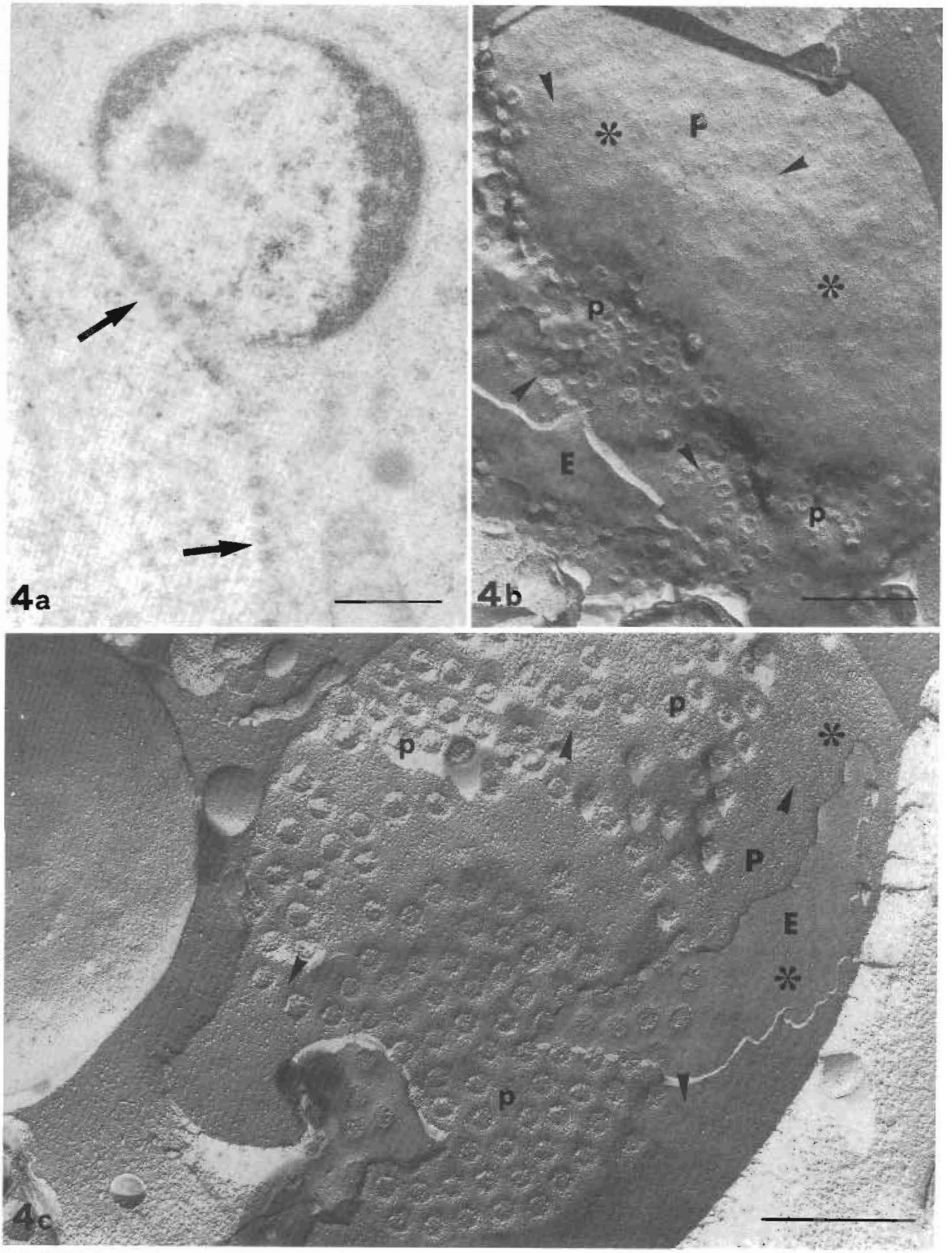

Fig. 4. *Caption on opposite page.*

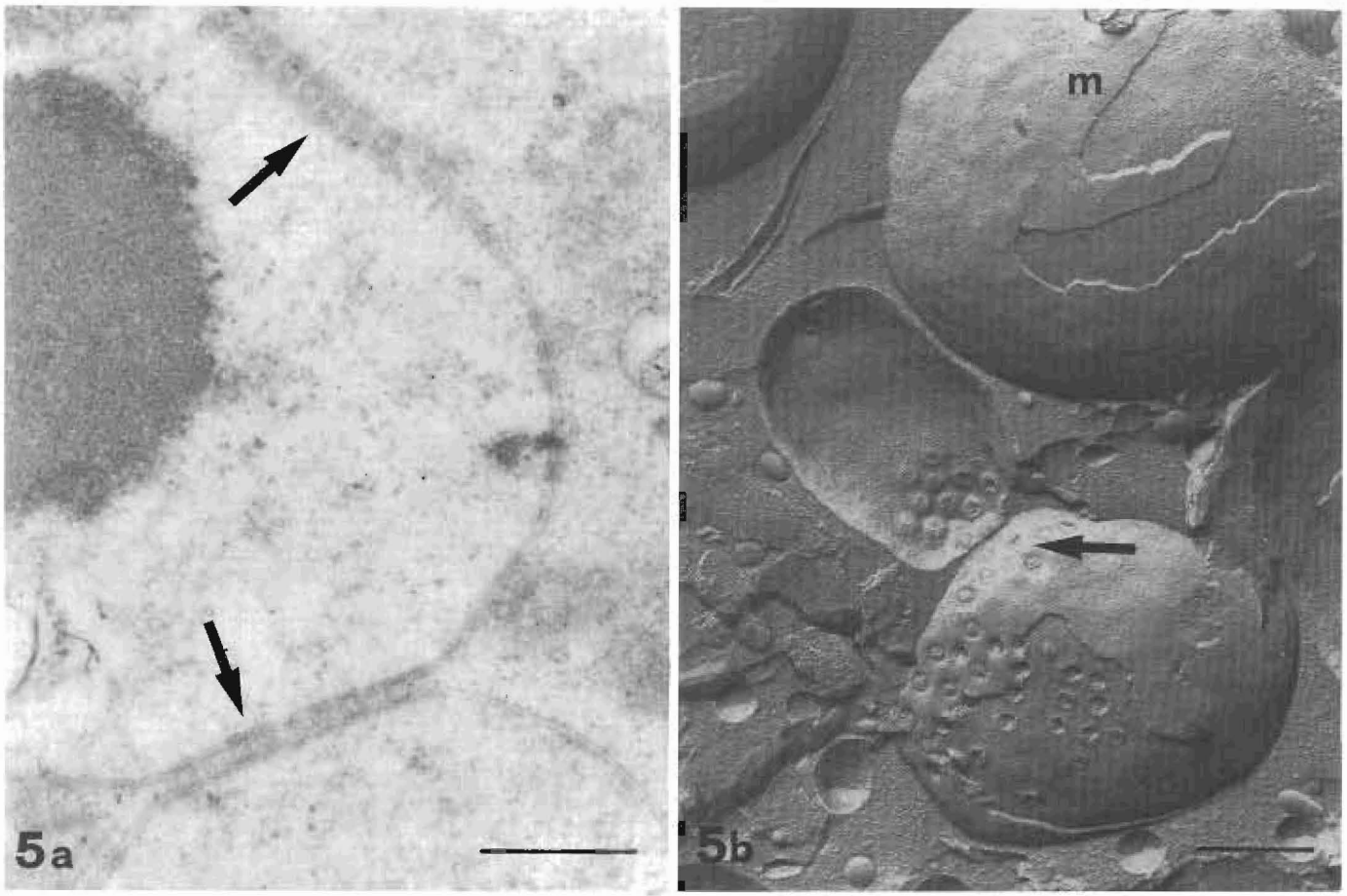

Fig. 5. (a–b) HL60 cells. Pore clusters appear localized between adjacent nuclear blebs (→) observed by conventional (a) and freeze-fracture electron microscopy (b). A pore-free micronucleus is also visible (**m**). Bar = 0.5 μm.

performed a cytochemical osmium-ammine reaction which revealed the presence of small amounts of DNA, concentrated in the two opposite nuclear poles, around pore cluster areas (Fig. 6c). Pore clustering in the course of the apoptotic phenomenon could also be observed in the staurosporine-treated MOLT-4 cells (Fig. 7a), as well as in the P815 cell exposed to hyperthermia (Fig. 7b). In this last model the chromatin marginations involved mostly the nuclear periphery, leaving small limited areas of diffuse chromatin in close relationship to the membrane. Only in these areas could pore complexes be shown, corresponding to the sticking points of the nuclear membranes which were otherwise sharply separated where pores were absent.

Discussion

The nucleoskeleton, currently named nuclear matrix, is clearly identifiable in the healthy interphase nucleus after chromatin digestion and different ionic force salt solution treatment (Martelli *et al.*, 1991). When studied by electron microscopy, it consists of a nucleolar remnant, a fibrillar network and a peripheral lamina which includes pore complexes (Falcieri *et al.*, 1992). The peripheral lamina is in close contact with the inner nuclear membrane and with intermediate filaments (Georgatos & Blobel, 1987), thus providing a continuous network connecting the cytoskeleton with the karyoskeleton. One significant role of the nuclear matrix is the maintenance of the spatial

Fig. 3 (a–c). Cap-shaped chromatin margination in apoptotic thymocytes (a) and TF-1 cells (b, c). Pore complex crowding (▶) appears around the diffuse chromatin areas while the opposite nuclear pole appears pore-free (→) and is frequently surrounded by strongly dilated cysternae (✻) (c). The inset shows the formation of *annulate lamellae*. **n** = nucleolus. Bar = 1 μm.

Fig. 4 (a–c) Nuclear pore distribution in apoptotic HL60 cells, observed by conventional (a) or freeze-fracture electron microscopy (b, c). They both appear in relationship to nuclear protrusions and cytoplasm (→), but constantly around areas of decondensed chromatin (a). Pore-free areas (✻) appear separated from pore clusters (**p**) (b, c), both displaying a regular distribution of intramembrane particles (▶). **P** = membrane P-face; **E** = membrane E-face. Bar = 0.5 μm.

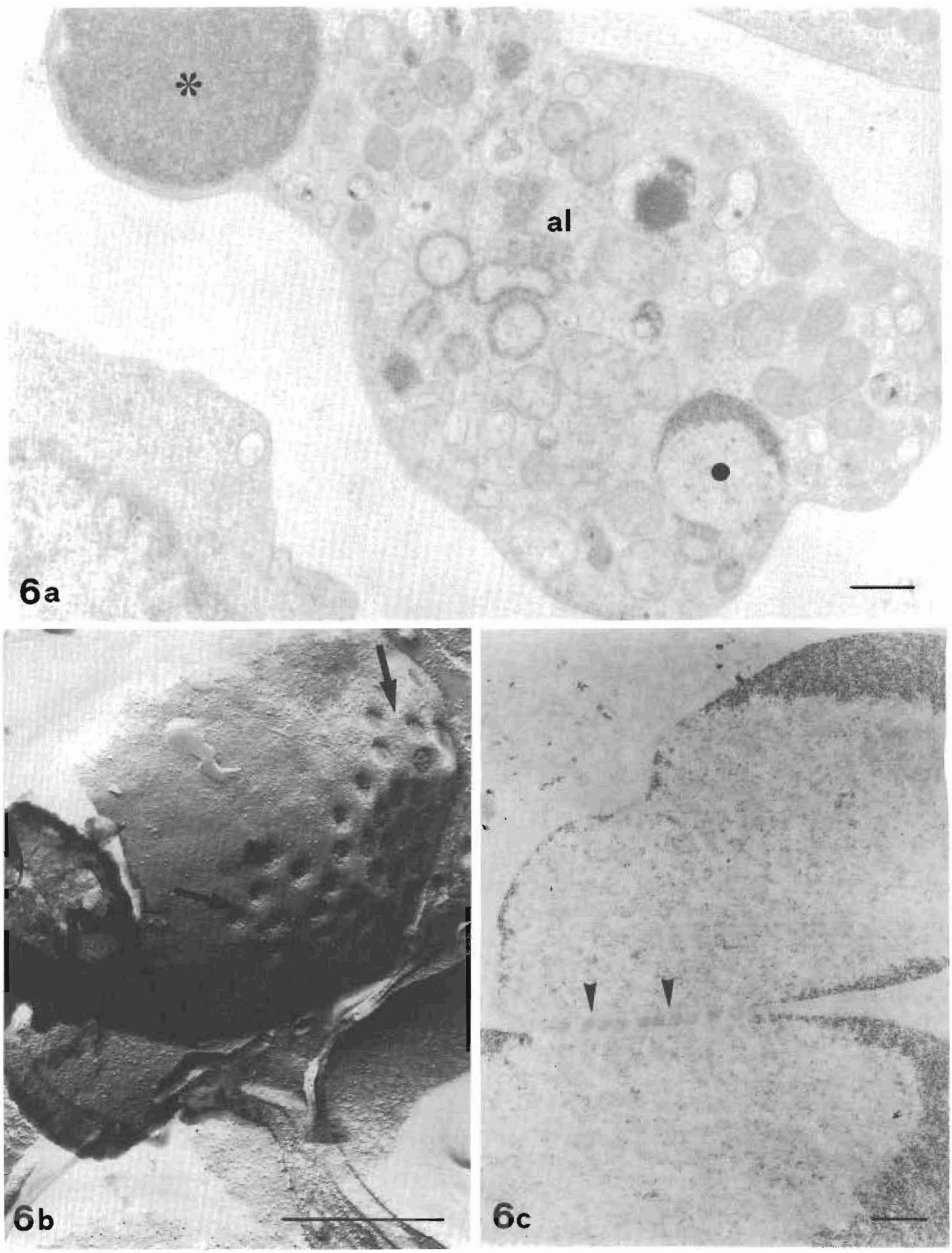

Fig. 6. *Caption on opposite page.*

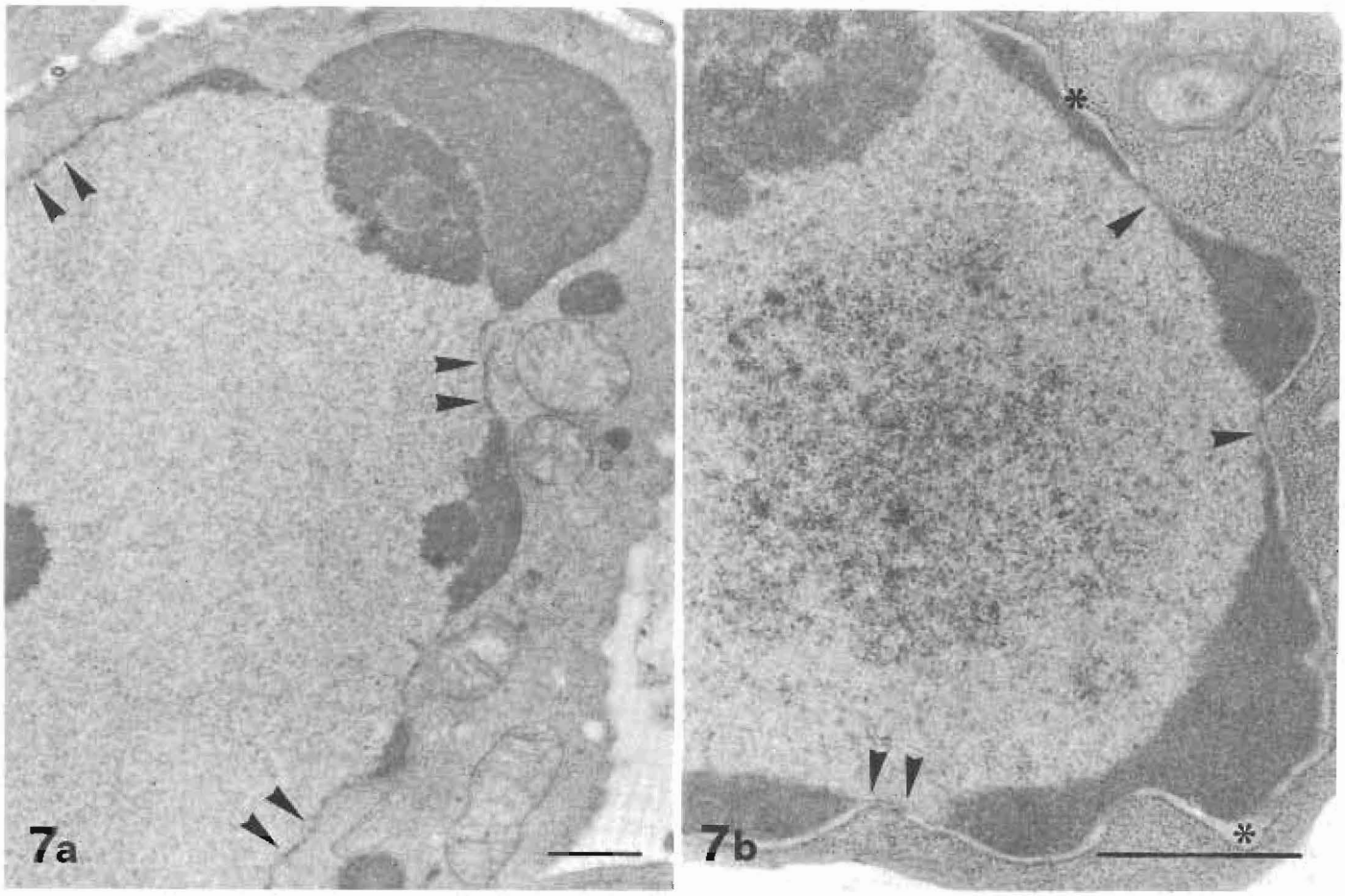

Fig. 7. (a–b). Apoptotic MOLT-4 (a) and P815 (b) cells. Pores appear localized in nuclear envelope areas adjacent to the decondensed chromatin (▶). Around the compact chromatin, in the absence of pores, the cysterna appears significantly dilated (✻). Bar = 1 μm.

distribution of the nuclear components (i.e. chromatin in its different arrangements, nucleolus and granules), as well as of the nuclear shape. This latter function is especially due to the peripheral lamina. It disappears during mitosis (Moir and Goldman, 1993) as well as in some apoptotic systems (Lazebnik *et al.*, 1993).

Despite the deep nuclear changes typical of apoptosis, the pore complexes can be recognized throughout the process. In contrast to those in the normal cell, the complexes have migrated and appear clustered in the nuclear membrane areas corresponding to the diffuse chromatin. However, no pores are demonstratable in the nuclear envelope portions surrounding the compact chromatin marginations or the cap-shaped structures. Interestingly, micronuclei, mostly containing condensed chromatin, do not show pores at all, or show only a small number of pores clustered together.

Variations of the nuclear pore complex distribution have occasionally been reported previously (Miller *et al.*, 1991) and it is now well known that their number and density per nucleus varies among cell types and experimental conditions. They appear to be generally independent of DNA content, nuclear surface and volume, but, in contrast, are correlated to nuclear activity (Carmo-Fonseca, 1982) and to the cell cycle (Conner *et al.*, 1980).

Particular structures related to nuclear pore formation are *annulate lamellae*. These are flattened cisternae, consisting of stacks of parallel membranes and containing dense pore complex aggregates which frequently appear in the cytoplasm of germ cells and in rapidly dividing somatic cells. They are commonly interpreted as the product of an excess of nuclear envelope precursor material (Dabauvalle *et al.*, 1991). In some of our apoptotic models, *annulate lamellae* could also be identified. Even if the cells which we examined were not rapidly dividing, a reduced utilization of nuclear envelope precursors is presumably required during the formation of micronuclei. The

Fig. 6. (a–c). HL60 cells. Micronuclei with homogeneous (✻) and cap-shaped (●) chromatin, as well as *annulate lamellae* (al) can be observed (a). Three-dimensional discrete distribution of nuclear pores (→) appears in a micronucleus (b). DNA osmium-ammine staining (c) displays prevalent DNA concentration at nuclear poles and a small amount of DNA close to the pores (▶) connecting the two nuclear formations. Bar = 0.5 μm.

assembling of *annulate lamellae*, close to the nuclear envelope surrounding diffuse chromatin areas, or scattered throughout the cytoplasm, could thus be explained.

In the course of apoptosis, we demonstrated constant nuclear pore migration. Areas of high pore concentration appear sharply separated from pore-free membrane portions, while no other membrane alteration seems to be present. During apoptosis, the nuclear membrane organization and ultrastructure appear closely comparable, both in conventional electron microscopy and freeze–fracture, to that of non-apoptotic cells, both in pore and pore-free domains. Therefore, this pore behaviour does not appear as a consequence of a modification of the apoptotic membrane but rather of some different mechanism.

A possible interpretation of pore migration during apoptosis may be made by considering the functional meaning of the degree of chromatin condensation. It has, in fact, been demonstrated that diffuse chromatin represents the DNA arrangement corresponding to active replication and transcription, while condensed chromatin is a temporaneously quiescent form (Maraldi *et al.*, 1982; Marinelli *et al.*, 1990). Nuclear pores mediate nuclear cytoplasmic traffic, and especially, the protein and ribonucleoprotein transport involved in transcriptional activity. Assuming that the clustered pores in the apoptotic nuclear membrane work properly, a functional role of their positioning can thus be hypothesized. Apoptotic cell metabolic activity is of relatively long duration, as biochemical data and the long morphological preservation of the cell demonstrate (Sorensen *et al.*, 1990). Exclusive pore clustering around the remaining diffuse chromatin areas might be due to the localization of residual nuclear activity in these areas. There could also be some physical force excluding the pores from the membranes above the condensing chromatin, presumably as a consequence of a rearrangement of the peripheral lamina.

Further information could be acquired by a high-resolution study of these pores and by a cytochemical analysis of their components, both now hampered by the relatively low percentage of apoptotic cells in any of our experimental models.

Acknowledgements

The authors are indebted to Dr Sandra Marmiroli, Istituto Citomorfologia Normale e Patologica CNR, Bologna and Dr Christine Betts, Dip. Patologia Generale, Università di Bologna, for their helpful contributions in DNA gel electrophoresis and in DNA osmium-ammine cytochemical staining. Mr Marcello Maselli is also thanked for his excellent photographic work, and Dr Frances Westall for her careful revision of the manuscript. The work was supported by CNR, P. F. ACRO, FATMA, MURST 60% Università di Chieti and Brescia and Istituti Ortopedici Rizzoli, Ricerca Corrente 1993.

References

ARENDS, M. J. & WYLLIE, A. H. (1991) Apoptosis: mechanisms and roles in pathology. *Int. Rev. Exp. Pathol.* **32,** 223–54.

ARENDS, M. J., MORRIS, R. G. & WYLLIE, A. H. (1990) Apoptosis: the role of the endonuclease. *Am. J. Pathol.* **136,** 593–608.

BOE, R., GJERTSEN, B. T., VINTERMYR, O. K., HOUGE, G., LANOTTE, M. & DOSKELAND, S. O. (1991) The protein phosphatase inhibitor okadaic acid induces morphological changes typical of apoptosis in mammalian cells. *Exp. Cell Res.* **195,** 237–46.

CARMO-FONSECA, M. (1982) Testosterone-induced changes in nuclear pore complex number of prostatic nuclei from castrated rats. *J. Ultrastruct. Res.* **80,** 243–51.

COLLINS, R. J., HARMON, B. V., GOBÈ, G. C. & KERR, J. F. R. (1992) Internucleosomal DNA cleavage should not be the sole criterion for identifying apoptosis. *Int. J. Radiat. Biol.* **61,** 451–3.

CONNER, G. E., NOONAN, N. E. & NOONAN, K. D. (1980) Nuclear envelope of chinese hamster ovary cells. Re-formation of the nuclear envelope following mitosis. *Biochemistry* **19,** 277–89.

DABAUVALLE, M. F., LOOS, K., MERKERT, H. & SCHEER, U. (1991) Spontaneous assembly of pore complex-containing membranes ('annulate lamellae') in *Xenopus* egg extract in the absence of chromatin. *J. Cell Biol.* **112,** 1073–82.

DARZYNKIEWICZ, Z., BRUNO, S., DEL BINO, G., GORCZYCA, W., HOTS, M. A., LASSOTA, P. & TRAGANOS, F. (1992) Features of apoptotic cells measured by flow cytometry. *Cytometry* **13,** 795–808.

DE LA TORRE, J., SUMNER, A. T., GOSALVEZ, J. & STUPPIA, L. (1992) The distribution of genes on human chromosomes as studied by in situ nick translation. *Genome* **35,** 890–3.

DERENZINI, M. & FARABEGOLI, F. (1990) Selective staining of nucleic acids by osmium–ammine complex in thin sections from Lowicryl-embedded samples. *J. Histochem. Cytochem.* **38,** 1495–501.

ELLIS, E. E., YUAN, J. & HORVITZ, H. R. (1991) Mechanism and functions of cell death. *Annu. Rev. Cell Biol.* **7,** 663–98.

FALCIERI, E., MARIANI, A. R., MARIANI, E., GOBBI, P., FACCHINI, A. & MANZOLI, F. A. (1990) A morphological study of membrane lesions during natural killer-mediated lysis. *J. Submicrosc. Cytol. Pathol.* **22,** 191–202.

FALCIERI, E., GOBBI, P., SABATELLI, P., SANTI, S., FARABEGOLI, F., RANA, R., CATALDI, A., MARALDI, N. M. & MARTELLI, A. M. (1992) A combined ultrastructural approach to the study of nuclear matrix thermal stabilization. *Histochemistry* **98,** 121–9.

FALCIERI, E., MARTELLI, A. M., BAREGGI, R., CATALDI, A. & COCCO, L. (1993) The protein kinase inhibitor staurosporine induces morphological changes typical of apoptosis in Molt-4 cells without concomitant DNA fragmentation. *Biochem. Biophys. Res. Comm.* **193,** 19–25.

FESUS, L., DAVIES, P. J. A. & PIACENTINI, M. (1991) Apoptosis: molecular mechanisms in programmed cell death. *Eur. J. Cell Biol.* **56,** 170–7.

GEORGATOS, S. D. & BLOBEL, G. (1987) Lamin B constitutes an intermediate filament attachment site at the nuclear envelope. *J. Cell Biol.* **105,** 117–25.

KAUFMANN, S. H. (1989) Induction of endonucleolytic DNA cleavage in human acute myelogenous leukemia cells by

etoposide, camptothecin, and other cytotoxic anticancer drugs: a cautionary note. *Cancer Res.* **49,** 5870–8.

KOURY, M. J. (1992) Programmed cell death (apoptosis) in Hematopoiesis. *Exp. Hematol.* **20,** 391–4.

LAZEBNIK, Y. A., COLE, S., COOKE, C. A., NELSON, W. G. & EARNSHAW, W. C. (1993) Nuclear events in apoptosis in vitro in cell-free mitotic extracts: a model system for analysis of the active phase of apoptosis. *J. Cell Biol.* **123,** 7–22.

LEDDA-COLUMBANO, G. M., CONI, P., CURTO, M., GIACOMINI, L., FAA, G., OLIVERIO, S., PIACENTINI, M. & COLUMBANO, A. (1991) Induction of two different modes of cell death, apoptosis and necrosis in rat liver after a single dose of thioacetamide. *Am. J. Pathol.* **139,** 1099–109.

MCCABE, M. J. JR. & ORRENIUS, S. (1992) Deletion and depletion: the involvement of viruses and environmental factors in T-lymphocyte apoptosis. *Lab. Invest.* **66,** 403–6.

MARALDI, N. M., CARAMELLI, E., CAPITANI, S., MARINELLI, F., ANTONUCCI, A., MAZZOTTI, G. & MANZOLI, F. A. (1982) Chromatin structural changes induced by phosphatidyl-serine liposomes on isolated nuclei. *Biol. Cell.* **46,** 325–8.

MARINELLI, F., FALCIERI, E., SQUARZONI, S., DEL COCO, R., ZINI, N., MANZOLI, L. & MARALDI, N. M. (1990) Image analysis of the chromatin organization in the nuclear domains of freeze fractured hepatocytes and lymphocytes. *Biol. Cell.* **70,** 107–19.

MARTELLI, A. M., FALCIERI, E., GOBBI, P., MANZOLI, L., GILMOUR, R. S. & COCCO, L. (1991) Heat induced stabilization of the nuclear matrix. A morphological and biochemical analysis in murine erythroleukemia cells. *Exp. Cell Res.* **196,** 216–25.

MILLER, M., PARK, M. K. & HANOVER, J. A. (1991) Nuclear pore complex: structure, function and regulation. *Physiol. Rev.* **71,** 909–49.

MOIR, R. D. & GOLDMAN, R. D. (1993) Lamin dynamics. *Curr. Opin. Cell Biol.* **5,** 408–11.

NIGG, E. A., BAEUERLE, P. A. & LUHRMANN, R. (1991) Nuclear import–export: in search of signals and mechanisms. *Cell* **66,** 15–22.

OBERHAMMER, F., FRITSCH, G., SCHMIED, M., PAVELKA, M., PRINTZ, D., PURCHIO, T., LASSMANN, H. & SCHULTE-HERMANN, R. (1993) Condensation of the chromatin at the membrane of an apoptotic nucleus is not associated with activation of an endonuclease. *J. Cell Sci.* **104,** 317–26.

SCHWARTZMAN, R. A. & CIDLOWSKI, A. (1993) Apoptosis: the biochemistry and molecular biology of programmed cell death. *Endocrine Rev.* **14,** 133–50.

SEN, S. & D'INCALCI, M. (1992) Biochemical events and relevance to cancer chemotherapy. *FEBS Lett.* **307,** 122–7.

SORENSEN, C. M., BARRY, M. A. & EASTMAN, A. (1990) Analysis of events associated with cell cycle arrest at G_2 phase and cell death induced by cisplatin. *J. Nat. Cancer Inst.* **82,** 749–55.

UCKER, D. S., OBERMILLER, P. S., ECKHART, W., APGAR, J. R., BERGER, N. A. & MEYERS, J. (1992) Genome digestion is a dispensable consequence of physiological cell death mediated by cytotoxic T lymphocytes. *Mol. Cell. Biol.* **12,** 3060–9.

VAUX, D. L. (1993) Toward an understanding of the molecular mechanism of physiological cell death. *Proc. Natl Acad. Sci. USA* **90,** 786–89.

VITALE, M., ZAMAI, L., MAZZOTTI, G., CATALDI, A. & FALCIERI, E. (1993) Differential kinetic of propidium iodide uptake in apoptotic and necrotic thymocytes. *Histochemistry* **100,** 223–9.

WYLLIE, A. H., KERR, J. F. R. & CURRIE, A. R. (1980) Cell death: the significance of apoptosis. *Int. Rev. Cytol.* **68,** 251–306.

ZAMAI, L., FALCIERI, E., ZAULI, G., CATALDI, A. & VITALE, M. (1993) The optimal detection of apoptosis by flow cytometry depends on cell morphology. *Cytometry* **14,** 891–7.

ZAULI, G., VITALE, M., RE, M. C., FURLINI, G., ZAMAI, L., FALCIERI, E., GIBELLINI, D., VISANI, G., DAVIS, B. R., CAPITANI, S. & LA PLACA, M. (1994) In vitro exposure to human immunodeficiency virus type-1 (HIV-1) induces apoptotic cells death of the factor-dependent TF-1 hematopoietic cell line. *Blood* **83,** 167–75.

ZYCHLINSKY, A., PREVOST, M. C. & SANSONETTI, P. J. (1992) Shigella flexneri induces apoptosis in infected macrophages. *Nature* **358,** 167–9.